

**THE EFFECT OF VARYING HDPE/PP BLEND COMPOSITION
ON THE CHARACTERISTICS OF THE MELT FLOW
OSCILLATING REGIMES**

Ms. Nattakamol Naiyakul

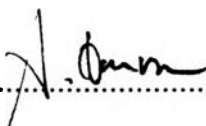
A Thesis Submitted in Partial Fulfillment of the Requirements
for the Degree of Master of Science
The Petroleum and Petrochemical College, Chulalongkorn University
in Academic Partnership with
The University of Michigan, The University of Oklahoma
and Case Western Reserve University

1997

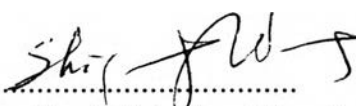
ISBN 974-636-179-1


Thesis Title : The Effect of Varying HDPE/PP Blend Composition on
the Characteristics of the Melt Flow Oscillating Regimes
By : Ms. Nattakamol Naiyakul
Program : Polymer Science
Thesis Advisors : Assoc. Prof. Shi Qing Wang
Assoc. Prof. Anuvat Sirivat

Accepted by the Petroleum and Petrochemical College, Chulalongkorn University, in partial fulfillment of the requirements for the Degree of Master of Science.


.....Director of the College
(Prof. Somchai Osuwan)

Thesis Committee


.....
(Assoc. Prof. Shi Qing Wang)


.....
(Assoc. Prof. Anuvat Sirivat)


.....
(Assoc. Prof. Kanchana Trakulcoo)

บทคัดย่อ

ณัฐกมล ไนยะกุล : อิทธิพลของโพลิเมอร์ผสมระหว่างโพลิเอทิลีนและโพลิโพรพิลีนที่มีต่อคุณสมบัติการไหลที่ไร้เสถียรภาพของโพลิเมอร์บนผิวขรุขระชนิด oscillation (The Effect of Varying HDPE/PP Blend Composition on the Characteristics of the Melt Flow Oscillating Regimes) อาจารย์ที่ปรึกษา : รศ.ดร. ชี ดิง หวัง และ รศ.ดร. อนุวัฒน์ ศิริวัฒน์ 106 หน้า ISBN 974-636-179-1

วิทยานิพนธ์ฉบับนี้เสนอการค้นคว้าและทดลองทางภาคปฏิบัติเกี่ยวกับอิทธิพลของโพลิเมอร์ผสมระหว่างโพลิเอทิลีนและโพลิโพรพิลีนที่มีต่อผิวขรุขระชนิด oscillation บนชิ้นส่วนพลาสติกที่ถูกรีดจากท่อกลม ผิวขรุขระชนิด oscillation เกิดจากการไร้เสถียรภาพในการไหล เนื่องจากโพลิเมอร์สูญเสียแรงยึดเหนี่ยวกับท่อกลม และสามารถไหลลื่นได้เมื่อค่าความเค้นของโพลิเมอร์ถึงจุดวิกฤต จุดวิกฤตของค่าความเค้นในผิวขรุขระชนิด oscillation เกิดในช่วง $3.29 - 3.25 (10^5 \text{ N/m}^2)$ จากการทดลองพบว่าความเร็วลื่นซึ่งมีความสัมพันธ์ต่อการเกิดผิวขรุขระชนิด oscillation และความยาวของการลื่นระหว่างโพลิเมอร์กับโลหะนั้น เปลี่ยนแปลงไปตามแรงเค้น และพบว่าปริมาณโพลิโพรพิลีนที่ถูกลดลงไปมีผลทำให้ความลื่นระหว่างโพลิเมอร์กับโลหะลดลง ดังนั้นความเร็วลื่น หรือความยาวของการลื่นระหว่างโพลิเมอร์กับโลหะจะน้อยลงไปด้วย ในท้ายที่สุดการเกิดผิวขรุขระชนิด oscillation จะถูกหยุดเอาไว้ จนกระทั่งถูกกำจัดออกไป ส่วนความยาวของการลื่นระหว่างโพลิเมอร์และโลหะนั้น พบว่าขึ้นอยู่กับอัตราส่วนของโพลิเมอร์ผสม ในทางตรงกันข้ามอัตราส่วนของโพลิเมอร์ผสมไม่มีผลต่อจุดวิกฤตของค่าความเค้นขีดข้อมูลที่ได้จากการวิจัยนี้จะเป็นประโยชน์ต่อความเข้าใจถึงที่มาของการเกิดผิวขรุขระซึ่งลดผลผลิต เพิ่มต้นทุนการผลิต และลดความสามารถในการประกอบชิ้นส่วนพลาสติกเล็ก ๆ

ABSTRACT

952011 : POLYMER SCIENCE PROGRAM

KEY WORD : WALL SLIP / STICK-SLIP TRANSITION / MELT FRACTURE/

EXTRAPOLATION LENGTH

NATTAKAMOL NAIYAKUL : THE EFFECT OF VARYING HDPE/PP

BLEND COMPOSITION ON THE CHARACTERISTICS OF THE

OSCILLATING REGIMES. THESIS ADVISORS : ASSOC. PROF. SHI

QING WANG AND ASSOC. PROF. ANUVAT SIRIVAT, 106 pp.

ISBN 974-636-179-1

This experiment aims at investigating the effect of varying HDPE/PP blend composition on the melt flow through a capillary in the oscillating regime. The oscillation regime is the result of some flow instability; it may originate when a polymer melt loses adhesion at the metallic wall and slip occurs when the wall shear stress exceeds a critical value. The critical wall shear stress, τ_w , of the oscillation regime occurs between 3.29 - 3.25 (10^5 N/m²). The slip velocity is found to vary linearly with the apparent strain rate, γ_a . Adding PP reduces the slippage between the polymer and metal surfaces, resulting in a smaller slip velocity or a smaller extrapolation length, b . The load oscillating regime is suppressed and eventually eliminated. The extrapolation length, b , varies linearly with HDPE content whereas the critical wall shear stress of the oscillating regime is independent of the blend composition. The slip data can be correlated with the extrudate skin defects. The extrapolation length was calculated to test the three possible regimes: entanglement, marginal and Rouse. The data provides some understanding of the origins of the extrudate distortions whose occurrences limit processing speed, increases operating cost, and reduces manufacturing capability.

ACKNOWLEDGMENTS

I would like to give special thanks to Assoc. Prof. Shi Qing Wang of Case Western Reserve University and Assoc. Prof. Anuvat Sirivat of The Petroleum and Petrochemical College, Chulalongkorn University, for their guidance throughout this work. I wish to express my special gratitude to The National Metal and Materials Technology Center (MTEC) for giving her financial support. Very special thanks are given to The Siam Chemical Trading Co., Ltd. and Thai Polyethylene Co., Ltd. for the raw materials of HDPE, PP and for providing a service for the density measurements.

Grateful appreciation is extended to Mr. Bernd - Udo Jacob and Mr. John W. Ellis for their help and useful suggestions on testing procedures. A special thank is extended to my family for giving love, encouragement and financial support.

Last but not least, I wish to express my special appreciation to the staff of the Petroleum and Petrochemical College and also to my friends in the Polymer Science Program.

TABLE OF CONTENTS

CHAPTER	PAGE
Title Page	i
Abstract	iii
Acknowledgments	v
Table of Contents	vi
List of Tables	ix
List of Figures	x
I INTRODUCTION	
1.1 Background	
1.1.1 Extrudate Distortions	2
1.1.2 Concept of Bifurcation	5
1.1.3 Stick - Slip Transition at Polymer Melt/Solid Interfaces	6
1.1.4 Theory of Brochard & de Gennes	7
1.1.5 Normalizations	8
1.2 Literature review	9
1.3 Objectives of Research	11
II EXPERIMENTAL DETAILS	
2.1 Materials	12
2.1.1 High Density Polyethylene (HDPE)	12
2.1.2 Polypropylene (PP)	12

CHAPTER	PAGE
2.2 Materials Preparation	12
2.2.1 Varying Composition of HDPE/PP (P340J) Blends	12
2.2.2 Varying Melt Flow Index of Two Grades of PP with a fixed HDPE	13
2.3 Instruments	13
2.3.1 Capillary Rheometer	13
2.3.2 Rheometer	14
2.3.3 Stereo Microscope	14
2.3.4 Optical Microscope	14
2.3.5 Melt Flow Index Meter	14
2.3.6 Differential Scanning Calorimeter (DSC)	15
2.3.7 Density Measurement	15
2.4 Characterization	16
2.4.1 Melt Flow Index Meter	16
2.4.2 Differential Scanning Calorimeter (DSC)	17
2.4.3 Density Measurement	18
2.4.4 Parallel Plate Rheometer	19
III RESULTS AND DISCUSSION	
3.1 Flow Curves	20
3.2 Surface Textures	27
3.3 Bifurcation Diagram	43
3.4 Wavelength	45
3.5 Slip Velocity	49
3.6 The Extrapolation Length	51

CHAPTER	PAGE
3.6.1 Effect of Composition	53
3.6.2 Effect of Melt Flow Index	54
3.7 Critical Parameters	55
3.7.1 Effect of Composition	55
3.6.2 Effect of Melt Flow Index	59
3.8 Normalizations	60
3.9 Viscosity	63
3.9.1 Steady State vs. Oscillatory State	63
3.9.2 The Power Law Index	67
IV CONCLUSIONS	68
REFERENCES	70
APPENDICES	72
CURRICULUM VITAE	106

LIST OF TABLES

TABLE	PAGE
2.4.1 Melt flow index	16
2.4.2 Melting temperature and percentage of crystallinity	17
2.4.3 Density	18
2.4.4 Glassy storage modulus	19
3.2.1 Surface texture of HDPE/PP blends	40
3.6.1 The asymptotic extrapolation length of each ratio	54
3.7.1 The critical parameter for each melt flow index in the oscillating regime	59
3.8.1 The recoverable shear of HDPE/PP (P340J) : 100/0	61
3.8.2 The recoverable shear (Asymptotic Values)	62
3.9.1 Power law index (n) and the constant value (K) of HDPE/PP (P340J) blends	67

LIST OF FIGURES

FIGURE	PAGE
1.1 Velocity field of stick - slip regime	7
1.2 The three regime of slip velocity in the plot between the extrapolation length	8
3.1 The wall shear stress, τ_w , versus the apparent strain rate, $\dot{\gamma}_a$, for HDPE/PP(P340J) blends of ratio 100/0	22
3.2 The wall shear stress, τ_w , versus the apparent strain rate, $\dot{\gamma}_a$, for HDPE/PP(P340J) blends of ratio 0/100	22
3.3 The wall shear stress, τ_w , versus the apparent strain rate, $\dot{\gamma}_a$, for HDPE/PP(P340J) blends of ratio 20/80	23
3.4 The wall shear stress, τ_w , versus the apparent strain rate, $\dot{\gamma}_a$, for HDPE/PP(P340J) blends of ratio 30/70	23
3.5 The wall shear stress, τ_w , versus the apparent strain rate, $\dot{\gamma}_a$, for HDPE/PP(P340J) blends of ratio 40/60	24
3.6 The wall shear stress, τ_w , versus the apparent strain rate, $\dot{\gamma}_a$, for HDPE/PP(P340J) blends of ratio 50/50	24
3.7 The wall shear stress, τ_w , versus the apparent strain rate, $\dot{\gamma}_a$, for HDPE/PP(P340J) blends of ratio 60/40	25
3.8 The wall shear stress, τ_w , versus the apparent strain rate, $\dot{\gamma}_a$, for HDPE/PP(P340J) blends of ratio 70/30	25
3.9 The wall shear stress, τ_w , versus the apparent strain rate, $\dot{\gamma}_a$, for HDPE/PP(P340J) blends of ratio 80/20	26
3.10 The wall shear stress, τ_w , versus the apparent strain rate, $\dot{\gamma}_a$, for HDPE/PP(P400S) blends of ratio 70/30	26

FIGURE	PAGE
3.11 Stereomicroscope photograph of the glossy smooth extrudate at HDPE/PP(P340J) : 100/0	28
3.12a Stereomicroscope photograph of the sharkskin surface at HDPE/PP(P340J) : 100/0	29
3.12b Optical microscope photograph of the sharkskin surface at HDPE/PP(P340J) : 100/0	29
3.13 Stereomicroscope photograph of the three form of the extrudate in the oscillating regime at HDPE/PP(P340J) : 100/0	30
3.14 Stereomicroscope photograph of the peeled orange extrudate at HDPE/PP(P340J) : 100/0	31
3.15 Stereomicroscope photograph of the melt fracture extrudate at HDPE/PP(P340J) : 100/0	31
3.16 Stereomicroscope photograph of the glossy smooth extrudate at HDPE/PP(P340J) : 0/100	32
3.17a Stereomicroscope photograph of a small peeled orange extrudate at HDPE/PP(P340J) : 0/100	33
3.17b Optical microscope photograph of the glossy smooth extrudate at HDPE/PP(P340J) : 0/100	33
3.18 Stereomicroscope photograph of the hazy smooth extrudate at HDPE/PP(P340J) : 70/30	35
3.19 Stereomicroscope photograph of the matteness extrudate at HDPE/PP(P340J) : 80/20	35
3.20 Stereomicroscope photograph of a ripple extrudate at HDPE/PP(P340J) : 70/30	36
3.21 Stereomicroscope photograph of a small scale roughness extrudate at HDPE/PP(P340J) : 60/40	36

FIGURE	PAGE
3.22 Stereomicroscope photograph of a helix extrudate extrudate at HDPE/PP(P340J) : 30/70	37
3.23a Stereomicroscope photograph of a ripple/hazy smooth extrudate at HDPE/PP(P340J) : 0/100	37
3.23b Stereomicroscope photograph of a melt fracture/ glossy smooth extrudate at HDPE/PP(P340J) : 0/100	38
3.24 Progressive effect of PP content on the blend skin textures	39
3.25 Flow curve of HDPE/PP : 100/0 blends	43
3.26 Hysteresis of the bifucation diagram of HDPE/PP (P340J): 100/0 in the oscillating regime	44
3.27 The wavelength, λ , versus the apparent strain rate, γ_a , in the oscillating regime of the HDPE/PP : 100/0 blends	46
3.28 The wavelength, λ , versus the apparent strain rate, γ_a , in the oscillating regime of the HDPE/PP : 80/20 blends	46
3.29 The wavelength, λ , versus the apparent strain rate, γ_a , in the oscillating regime of the HDPE/PP : 70/30 blends	47
3.30 The wavelength ratio versus the apparent strain rate, γ_a , in the oscillating regime of the HDPE/PP : 100/0, 80/20 and 70/30 blends	48
3.31 The slip velocity, V_s , versus the apparent wall strain rate corrected for slip, $\gamma_{a,s}$, in the oscillating regime	50
3.32 The extrapolation length, b , versus the apparent wall strain rate corrected for slip, $\gamma_{a,s}$, in the oscillating regime	51
3.33 The extrapolation length, b , versus the slip velocity, V_s , for HDPE/PP (P340J) blends in the oscillating regime	52

FIGURE	PAGE
3.34 Composition effect on the asymptotic extrapolation length, b_{∞} , for HDPE/PP (P340J) blends	53
3.35 Composition effect in the critical wall shear stress, $\tau_{w,c}$, of HDPE/PP(P340J) blends in the oscillating regime	55
3.36 Composition effect in the critical apparent strain rate, $\gamma_{a,c}$, of HDPE/PP(P340J) blends in the oscillating regime	56
3.37 Composition effect in the critical wall shear stress, τ_w , of HDPE/PP(P340J) blends in the melt fracture regime	57
3.38 Composition effect in the critical apparent strain rate, $\gamma_{a,c}$, of HDPE/PP(P340J) blends in the melt fracture regime	58
3.39 The master curve of HDPE/PP(P340J) : 100/0	60
3.40a Comparison of the capillary viscosity vs. the apparent strain rate and the parallel plate viscosity vs. the apparent wall strain rate corrected for the HDPE/PP (P340J) : 100/0	65
3.40b Comparison of the capillary viscosity vs. the apparent strain rate and the parallel plate complex viscosity vs. the frequency for the HDPE/PP (P340J) : 100/0	65
3.41a Comparison of the capillary viscosity vs. the apparent strain rate and the parallel plate viscosity vs. the apparent wall strain rate corrected for the HDPE/PP (P340J) : 0/100	66
3.40b Comparison of the capillary viscosity vs. the apparent strain rate and the parallel plate complex viscosity vs. the frequency for the HDPE/PP (P340J) : 0/100	66
B.1 Flow curve of HDPE/PP : 80/20 blends	100

B.2	Flow curve of HDPE/PP : 70/30 blends	100
B.3	Flow curve of HDPE/PP : 60/40 blends	101
B.4	Flow curve of HDPE/PP : 50/50 blends	101
B.5	Flow curve of HDPE/PP : 40/60 blends	102
B.6	The reduced storage modulus of HDPE/PP(P340J) : 80/20	102
B.7	The reduced storage modulus of HDPE/PP(P340J) : 70/30	103
B.8	The reduced storage modulus of HDPE/PP(P340J) : 60/40	103
B.9	The reduced storage modulus of HDPE/PP(P340J) : 50/50	104
B.10	The reduced storage modulus of HDPE/PP(P340J) : 40/60	104
B.11	The reduced storage modulus of HDPE/PP(P340J) : 30/70	105
B.12	The reduced storage modulus of HDPE/PP(P340J) : 20/80	105